

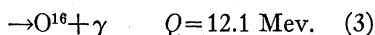
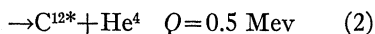
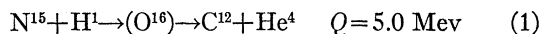
The Disintegration of N^{15} by Protons*

ALOIS SCHARDT, WILLIAM A. FOWLER, AND CHARLES C. LAURITSEN
Kellogg Radiation Laboratory, California Institute of Technology, Pasadena 4, California
 (Received February 8, 1951)

The absolute cross sections of the reactions (1) $N^{15}(p, \alpha)C^{12}$, (2) $N^{15}(p, \alpha\gamma)C^{12}$, and (3) $N^{15}(p, \gamma)O^{16}$ have been measured from 0.2 to 1.6 Mev. The thick target yield of reaction (1) was also measured at 0.100 Mev. Resonances were found at 0.338, 1.05, and 1.210 Mev for reaction (1); at 0.429, 0.898, 1.210, and possibly 1.05 Mev for reaction (2); and at 1.05 Mev for reaction (3). Most of the resonances follow closely the shape of the single level dispersion formula. The 1.05-Mev resonance is asymmetric and cannot be explained as easily. The cross section of reaction (1) has been extrapolated to stellar energies and is given by $\sigma = (110/E) \times \exp(-6.95E^{-1/2})$ barns for E in Mev in the energy region near 0.030 Mev.

I. INTRODUCTION

ON bombardment of N^{15} with protons of energy below 2 Mev the following reactions are energetically possible:



The first to observe reaction (1) were Burcham and Smith.¹ They bombarded a mixture of oxygen and nitrogen with 0.5-Mev protons. The alpha-particle group found varied in intensity with the nitrogen content and had approximately the correct energy. Fowler, Lauritsen, and Lauritsen^{2,3} observed reaction (2) for proton energies between 0.6 and 1.4 Mev. They measured the quantum energy to be 4.5 Mev and found resonances at 0.88, 1.03, and 1.20 Mev. Tangen⁴ observed a gamma-ray resonance at 0.428 Mev which he attributed to reaction (3).⁵

Measurement of the absolute cross sections of these reactions became of interest when Bethe⁶ investigated the carbon-nitrogen cycle as a source of stellar energy. For his calculations it was necessary to know the cross sections at stellar energies, near 30 kev. Holloway and Bethe⁷ measured the cross sections of reaction (1) near 360 kev, but did not measure the bombarding energy with great accuracy. Cochrane and Hester⁸ measured the excitation of reaction (1) from 0.2 to 0.5 Mev and found a resonance near 0.4 Mev.

In order to extrapolate the cross sections from the energy at which they are measured to stellar energies it is desirable to know the excitation curves of the reac-

tions in some detail. We have measured the yield of alpha-particles and quanta from the disintegration of N^{15} by protons from 0.2 to 1.6 Mev. Two groups of alpha-particles corresponding to reactions (1) and (2) were found. At most of the resonances only 4.5-Mev radiation was present. However, at 1.05-Mev coincidence absorption measurements showed the presence of 13-Mev radiation. As reaction (1) is of primary interest in connection with stellar energy production, its yield was also measured at 0.10 Mev to check the extrapolation.

The excitation curves give information about the nature and frequency of levels in the compound nucleus, O^{16} . The levels formed are at an excitation energy between 12.1 and 13.6 Mev in O^{16} . The presence of only one short range alpha-particle group indicates that no level in C^{12} below 4.5 Mev is produced in these reactions. From the cross sections and experimental widths at the resonances approximate widths for alpha-particle and gamma-ray emission can be calculated. However, an accurate analysis has to wait until angular distribution and correlation measurements now underway in this laboratory are concluded. As these angular distribution measurements of the reaction products have not yet been completed, the results are most conveniently expressed as 4π times the differential cross sections per unit solid angle in the direction of observation.

II. EXPERIMENTAL ARRANGEMENT

A solid nitrogen compound enriched with N^{15} was bombarded with mono-energetic protons and the yield of alpha-particles and quanta was measured as a function of proton energy. For most of the work the protons were accelerated by the 1.6-Mev pressure insulated electrostatic accelerator of the California Institute of Technology.³ An electrostatic analyzer,⁹ calibrated with the 873.5-kev $F^{19}(p, \alpha\gamma)$ resonance, held the proton energy within 0.02 percent. The H^+ beam was used from 0.4 to 1.6 Mev and the HH^+ and HHH^+ beams from 0.2 to 0.4 Mev. The target arrangement described by Snyder *et al.*¹⁰ was used. Above bombarding energies

* This work was assisted by the joint program of the ONR and AEC.

¹ W. E. Burcham and C. L. Smith, *Nature* **143**, 795 (1939).

² W. A. Fowler and C. C. Lauritsen, *Phys. Rev.* **58**, 192 (1940).

³ Lauritsen, Lauritsen, and Fowler, *Phys. Rev.* **59**, 241 (1941).

⁴ R. Tangen, *Kgl. Norske. Videnskabs Selskabs Skr.* No. 1 (1946).

⁵ Our results indicate that this resonance is due to reaction (2).

⁶ H. A. Bethe, *Phys. Rev.* **55**, 103, 434 (1939); and *Astrophys. J.* **94**, 37 (1940).

⁷ M. G. Holloway and H. A. Bethe, *Phys. Rev.* **57**, 747 (1940).

⁸ W. Cochrane and A. G. Hester, *Proc. Roy. Soc. (London)* **199**, 458 (1949).

⁹ Fowler, Lauritsen, and Lauritsen, *Rev. Sci. Instr.* **18**, 818 (1947).

¹⁰ Snyder, Rubin, Fowler, and Lauritsen, *Rev. Sci. Instr.* **21**, 852 (1950).

of 0.85 Mev a magnetic spectrograph,¹⁰ capable of focussing 2-Mev alpha-particles, was used to separate the long-range alpha-particles from the elastically scattered protons. It detected particles emitted at 138° with the incident beam. A thin mica foil mounted in the foil holder of the target chamber slowed the alpha-particles down from about 5 to below 2 Mev. Below 0.85 Mev, a proportional counter at 90° with the beam was substituted for the spectrograph because a larger solid angle was needed to compensate for the decrease in yield. The counter window, 0.317 inches in diameter, was 0.800 inches from the center of the target spot and thus subtended 0.12 steradians.

The quanta were detected using a Geiger-Müller counter coincidence arrangement^{11,12} at 90° with the beam. The counters made by Radiation Counter Laboratories of Chicago, have an effective length of $3\frac{3}{8}$ inches and a diameter of $23/32$ inch. The wall thickness is 30 mg/cm² of glass plus a thin silver deposit. The two rear counters were 0.75 inches from the front counter, which in turn was 1.50 inches from the target. This corresponds to poor geometry and the solid angle has to be found empirically. At a strong resonance the yield was measured in this position and also with the counter 4.0 inches from the target. In the latter position the solid angle can be calculated using standard formulas.¹¹ The ratio of the readings then was used to determine the solid angle in the near position.

For the 0.10-Mev measurement the low voltage accelerator and high current ion source described by Hall *et al.*^{13,14} were used. A horizontal section through the target arrangement is shown in Fig. 1. The long range alpha-particles were detected with a proportional counter. Its aperture was 0.700 inches from the center of the target. Apertures 0.532 and 0.750 inches in diameter were used, giving solid angles of 0.40 and 0.75 steradians. Air cooling of the target support was neces-

sary as 10 watts had to be dissipated. To reduce the deposition of carbon by the beam, a liquid air trap was provided as shown.

III. TARGETS

The choice of target material was primarily dictated by the availability of compounds enriched with N¹⁵. The most suitable compound we could find was KNO₃, which is available from the Eastman Kodak Company enriched to 61 percent N¹⁵. The proton disintegration cross sections of potassium, N¹⁴, and oxygen are sufficiently small as not to interfere with the N¹⁵ measurements. KNO₃ decomposes at 400°C but will evaporate in vacuum at a slightly lower temperature. To show that it does not decompose in the evaporation, a thin target deposited on a silver leaf was analyzed with elastically scattered protons¹⁰ and the results compared with those using a thick target of the material before evaporation.

It was possible to evaporate targets of any desired thickness onto a copper target holder. It was found that the target decomposed under prolonged bombardment by the proton beam ($\sim 0.2\mu\text{a}$). The loss of nitrogen was assumed to be proportional to the total charge collected. The rate of loss was checked frequently by comparing yields at selected bombarding energies. The current density of the proton beam was not constant over the target area; therefore, the central part lost nitrogen more quickly. Since the beam wandered slightly, the yield showed appreciable fluctuations and the target had to be replaced frequently.

The energy-equivalent target thickness in kev was always measured at the 0.898-Mev resonance, either by width at half maximum or by the area under the curve. The accuracy of this measurement was about ± 10 percent. The result was converted into a number of N¹⁵ atoms by dividing the width by the stopping cross section per N¹⁵ nucleus. For KNO₃ enriched to 61 percent N¹⁵ this cross section is equal to 5.57×10^{-17} kev cm at 0.90 Mev. On all graphs in this report the target thickness is given at 0.90 Mev.

For the measurement at 0.10 Mev a more stable nitrogen compound was needed. Titanium nitride was prepared by heating a pellet of sintered titanium metal in an atmosphere of enriched ammonia.¹⁵ The surface layer was analyzed with elastically scattered protons.¹⁰ Light scattering nuclei were indicated by steps or peaks superimposed on the thick target scattering curve of titanium. The measurements indicated that there was some oxygen in the surface; probably a layer a fraction of a kev thick. The concentration of nitrogen was smaller than corresponds to TiN. A comparison of the quantum yield at the 0.898-Mev resonance between KNO₃ and this target showed that the surface layer had only $\frac{2}{3}$ as much nitrogen as expected in the compound TiN.

¹⁵ The authors are greatly indebted to Professor Don Yost, Dr. David L. Douglas, and Mr. Sidney Gibbons for suggesting this compound and preparing the targets.

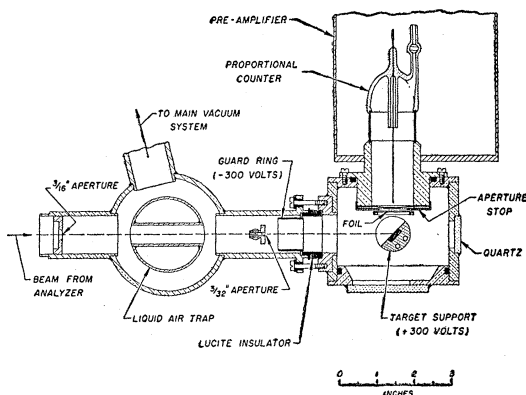


Fig. 1. Experimental arrangement used in the 0.100-Mev measurement of long-range alpha-particles.

¹¹ Fowler, Lauritsen, and Lauritsen, *Revs. Modern Phys.* **20**, 236 (1948).

¹² Fowler, Lauritsen, and Tollestrup, *Phys. Rev.* **76**, 1767 (1949).

¹³ R. N. Hall, *Rev. Sci. Instr.* **18**, 703 (1947).

¹⁴ R. N. Hall and W. A. Fowler, *Phys. Rev.* **77**, 197 (1950).

Another difficulty encountered with this target was the presence of a slight boron contamination. The $B^{11}(p, \alpha)2He^4$ reaction produces alpha-particles in the same energy range as $N^{15}(p, \alpha)C^{12}$. At 0.10 Mev a compressed amorphous boron target gave more than 10^4 times the yield of TiN^{15} . To measure the effect of this contamination, a titanium pellet was nitrided with ordinary nitrogen. The two targets were prepared under identical circumstances and were washed together in the same solutions. Thus, it may be assumed that the same amount of boron was on or in both targets. Different spots on the same target gave consistent results. About twice as many counts were observed with the enriched target as with the normal TiN target.

IV. OBSERVATIONS OF THE LONG-RANGE ALPHA-PARTICLES

At 100 kev the energy variation of the cross sections is primarily determined by the Gamow penetration factor. Neglecting the effects of resonance factors, Hall and Fowler¹⁴ have derived an expression for the cross section using the thick target yield:

$$\sigma = \frac{0.993\epsilon Z_0 Y}{2E^{\frac{1}{2}}} \left(1 + \frac{E^{\frac{1}{2}}}{Z_0} + \dots \right) \text{cm}^2, \quad (1)$$

where E is the proton energy in Mev, Y the thick target yield in disintegrations per proton, ϵ the stopping cross sections per active nucleus in Mev cm^2 , and Z_0 the atomic number of the target nucleus. At 100 kev the stopping cross section of TiN is 3.8×10^{-20} Mev cm^2 per nitrogen atom and is thus 5.7×10^{-20} Mev cm^2 for the targets we employed, since only $\frac{2}{3}$ titanium in the surface layer had been converted into TiN . The target was enriched to 31.5 percent with N^{15} so that $\epsilon = 1.8 \times 10^{-19}$ Mev cm^2 per N^{15} atom. From the observed yield, we calculated that $\sigma = 5 \times 10^{-7}$ barns at 101.5 kev. The actual bombarding energy was slightly lower (~ 2 kev) because of the thin oxide layer on the target. The uncertainty in determining the effect of the boron contamination limits the accuracy to about 50 percent. Statistical and geometric errors are negligible compared to this.

Up to bombarding energies of 0.85 Mev the alpha-particles were counted at 90° to the beam with a proportional counter. The effective cross section was determined using a thin target (2-kev equivalent thickness at 0.9-Mev proton energy or 7 kev at 0.2 Mev). However, below 0.25 Mev a target 60-kev thick at 0.90 Mev was used to increase the yield. The slope of the yield curve was used to compute the effective cross section. A small correction of at most 10 percent was made in converting the semi-thick target slope into the thick target slope used in computing the cross section.

Above 0.85 Mev, the bombarding energy at which proton and alpha-particle ranges became equal, separation of scattered protons and alpha-particles was accomplished with the magnetic spectrograph. Since

its maximum field cannot deflect alpha-particles of greater than 2 Mev into the counter, mica foils of 1.69 and 2.00 cm air equivalent were mounted on a foil holder and could be turned in front of the spectrograph as needed. The foils were calibrated using protons scattered by a thin silver foil. The proton energy (1.190 Mev) was chosen to give the same velocity as the velocity of the long-range alpha-particles. The number of protons scattered into the spectrograph with and without the mica foils was the same with 5 percent. The displacement of the proton peak gave the energy loss in the mica foil. The width of the peak gave the straggling.

The alpha-particle yield was measured by the method described by Brown *et al.*¹⁶ At intervals of 0.12 Mev an alpha-profile curve¹⁷ was taken. The number of doubly charged alpha-particles entering the spectrograph is then given by

$$n(He^{++}) = 1.602 \times 10^{-13} \frac{R}{q} \int \frac{N(I)}{I} dI. \quad (2)$$

In this equation $R = P/\delta p$ is the momentum resolution of the spectrograph and $N(I)$ is the number of alpha-particle counts at a given magnetometer¹⁸ current I , for a charge of q microcoulombs of protons. As long as the shape of the profile curve is determined primarily by the straggling in the mica foil one would expect that the quantity, η , defined by

$$\eta = \frac{1}{N_{\max}} \int \frac{N(I)}{I} dI \quad (3)$$

would be a constant. This proved to be the case within the experimental error of 5 percent. For a 25-kev target $\eta = 0.0605$ with foil No. 1 (1.69 cm of air) and $\eta = 0.106$ with foil No. 2 (2.00 cm of air). Thus, at intermediate points only, the maximum value, N_{\max} , on the profile curve had to be measured.

The formula used in computing the cross section was as follows:¹⁶

$$\sigma_{\text{eff}} = \frac{1.602 \times 10^{-13}}{qnt} \frac{4\pi R}{\Omega_L} \left(\frac{d\Omega_C}{d\Omega_L} \right)^{-1} \left(1 + \frac{n(He^+)}{n(He^{++})} \right) \eta N_{\max},$$

where nt is the number of N^{15} atoms per cm^2 of target, Ω_L and Ω_C are the acceptance solid angles of the spectrograph in laboratory and center-of-mass systems, respectively, while $n(He^+)/n(He^{++})$ is the ratio of singly to doubly charged alpha-particles entering the magnet. The ratio was determined as described in reference 16.

The effective cross section computed in this way is not greatly distorted by the target thickness, since the

¹⁶ Brown, Snyder, Fowler, and Lauritsen, *Phys. Rev.* **82**, 159 (1951).

¹⁷ At a fixed bombarding energy the alpha-particles are counted as a function of magnetic field to yield a "profile" curve.

¹⁸ C. C. Lauritsen and T. Lauritsen, *Rev. Sci. Instr.* **19**, 916 (1948).

target used was 25 kev thick. Only at the 1.21-Mev resonance is a correction for target thickness necessary. Here the resonance cross section was calculated by assuming that the half width is the same for both long- and short-range alpha-particles.

The accuracy is limited primarily by target deterioration. With the exception of the region 1.3 to 1.6 Mev at least 100 and generally over 500 counts were taken at each point; thus statistical errors are small. The data taken with the proportional counter are more consistent because less bombardment was needed for the desired number of counts. In the region where proportional counter and spectrograph data overlap, the agreement (see Fig. 6 which is discussed in Part VII) is better than might be expected, especially since the data correspond to two different angles of observation. The stopping cross section enters into all computations. It has not been measured for potassium and interpolation between measured elements is probably only good to 10 percent. Thus the over-all accuracy is approximately 15 percent.

Cochrane and Hester⁸ have measured the long-range alpha-cross section from 0.2 to 0.5 Mev. Within experimental errors the shape of their excitation curve agrees with our results. However, their cross section at the low resonance is only 0.013, compared to 0.09 barn obtained in this investigation. This discrepancy is not too surprising if one considers the difficulties associated with nitrogen targets, especially since only small quantities of separated isotopes are available. Cochrane and Hester started with $N^{15}H_4N^{14}O_3$ and transformed it by

Kjeldahl's method into NH_4Cl . From this they evolved NH_3 for use in a gas target. The amount of $N^{15}H_4NO_3$ available to them was sufficient for only one target and no check could be made on the efficiency of the chemical process. On the other hand, we were able to use $KN^{15}O_3$ which had been analyzed by the Eastman Kodak Company. Three different KNO_3 targets gave consistent results and agree with preliminary data taken with the TiN target.

V. OBSERVATIONS OF THE GAMMA-RADIATION

The singles counts from the front counter of the coincidence arrangement together with the efficiency curves similar to those given by Fowler, Lauritsen, and Lauritsen¹¹ were used in computing quantum yields. A revised efficiency curve for counters and electroscopes with aluminum walls will be published in the near future. The counter efficiency is 3.0 percent for 4.5-Mev quanta and 9.7 percent for 13-Mev radiation. The absorption of the gamma-radiation in the converter and target chamber was calculated using the absorption coefficients of Streib.¹⁹ This correction amounted to 10 percent and 7 percent for the 4.5- and 13-Mev quanta.

Absorption of secondaries was measured by the coincidence counts using different absorber thickness between the counters (Fig. 2). To interpret these data, curves similar to Fig. 10 in Fowler *et al.*¹¹ were prepared for the geometric arrangement used. From these curves it was possible to fit semi-empirical curves to the $N^{15}+H^1$ data. The curves taken at the 0.43- and 0.90-Mev resonances are consistent with simple 4.5-Mev radiation. The points taken at 1.05 Mev can be fitted best by assuming that 4 percent of the radiation has an energy of 13 Mev. The slope of curve (b) or (c) of Fig. 2 in the 9- to 16-mm region is typical of 13-Mev gamma-rays. Unfortunately the standard curves are not very accurate and thus the quantum energy may fall anywhere between 11 and 15 Mev. From mass differences the energy of the capture radiation leading to the ground state in O^{16} is 13 Mev. Furthermore curve (c) of Fig. 2 shows that cascade radiation cannot be ruled out entirely.

To measure the excitation curve of the hard component, coincidence counts were measured with 8.9 mm of aluminum absorber. On a typical run the background amounted to 4 counts out of 25. To check this excitation curve, a coincidence absorption curve was also taken at 1.12-Mev bombarding energy. It showed the expected decrease in hard quanta.

The accuracy of gamma-ray cross sections cannot be as high as that for alpha-particles. There is always an uncertainty in the Geiger counter efficiency and its sensitive volume. Measurements on the thick target yield at the 0.898-Mev resonance varied as much as 15 percent. The solid angle measurement at the $1\frac{1}{2}$ -inch position is only accurate to 10 percent. Thus the over-all

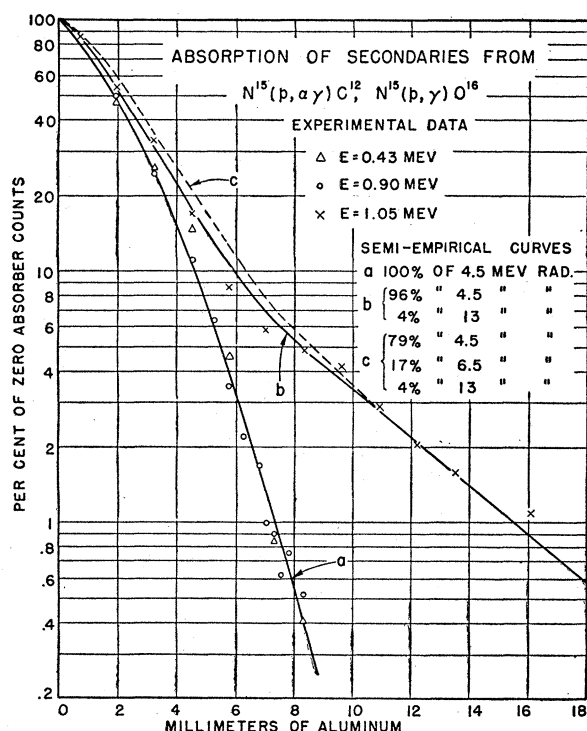


FIG. 2. Absorption of the secondaries[†] produced in a thick aluminum converter by the $N^{15}(p, \gamma)$ radiations.

¹⁹ Streib, Fowler, and Lauritsen, Phys. Rev. **59**, 253 (1941).

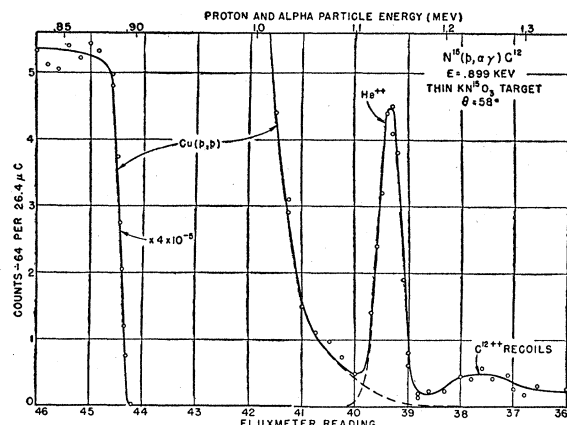


FIG. 3. Profile curve of alpha-particles from $N^{15}(p, \alpha \gamma)C^{12}$ and fluxmeter calibration using protons elastically scattered from a clean copper surface.

accuracy is about 20 percent for the 4.5-Mev quanta and somewhat poorer for the hard component. At the 0.898-Mev resonance the short range alpha-particles were measured at 58° simultaneously with the gamma-rays at 90° . The ratio turned out to be 0.85 alphas per quantum. The deviation from one alpha per quantum is not unexpected in view of the possibility that the angular distribution of the alpha-particles is not isotropic. The position of the two sharp resonances 0.429 and 0.898 Mev is accurate to 1 kev, since they were compared directly with the 0.8735-Mev F^{19} resonance.

VI. OBSERVATIONS OF THE SHORT-RANGE ALPHA-PARTICLES

The yield of alpha-particles from $N^{15}(p, \alpha \gamma)C^{12}$ was large enough at the 0.898- and 1.210-Mev resonances for observation with the spectrograph. In the backward direction the alpha-particles are focused by approximately the same magnetic field as the elastically scattered protons. However, by observing at 58° , it was possible to separate the two groups. Figure 3 shows the profile curve for a thin KNO_3 target bombarded with 0.899-Mev protons. For positive identification of the alpha-particles, their excitation curve was measured simultaneously with that of the gamma-rays at the 0.898-Mev resonance [Fig. 4(a)] and the curves were found to be identical. Also as noted above, the alpha-particle and quantum yields agree within experimental error.

In computing the alpha-particle energy, the midpoint of the front slope of the profile curve is generally taken to correspond to alpha-particles produced at the surface of the target. But the 0.898-Mev resonance is only 2.25-kev wide in terms of the bombarding proton energy, thus the alpha-particle spread (~ 10 kev) even with a thick target is not enough to fill the spectrograph window. A detailed analysis was made by folding the spectrograph window into the known yield of alpha-particles as a function of energy and fitting the ob-

served and calculated curves. This fitting furnished the energy of the alpha-particles produced by the protons at resonance. The Q -value of the reaction was then computed using the standard nonrelativistic formula. From the three independent measurements at the 0.898-Mev resonance the following values were obtained: 0.5281, 0.5361, and 0.5302 Mev. At the 1.210-Mev resonance, 0.5226 Mev was measured. This is probably not as accurate as the results at the lower resonance because the scattered protons interfered slightly with the alpha-particle measurements. The average is 0.529 Mev. The angle of observation was measured to within $\pm \frac{1}{2}^\circ$. This together with other systematic errors gives an uncertainty of ± 8 kev so that $Q^* = 0.529 \pm 0.008$ Mev.

VII. RESULTS AND DISCUSSION

The over-all picture of the cross sections is given in Fig. 5. For graphical purposes the width of the two narrow resonances (at 0.429 and 0.898 Mev) has not been drawn to scale. Details of the curves with experimental points are given in Figs. 4, 6, and 7. The curves give 4π times the cross section per unit solid angle in the direction of observation. All gamma-ray measurements were made at 90° , as were the long-range alpha-particles up to 0.85 Mev. Between 0.7 and 1.6 Mev the long-range alpha-particles were observed at 137.8° with the incident proton beam.

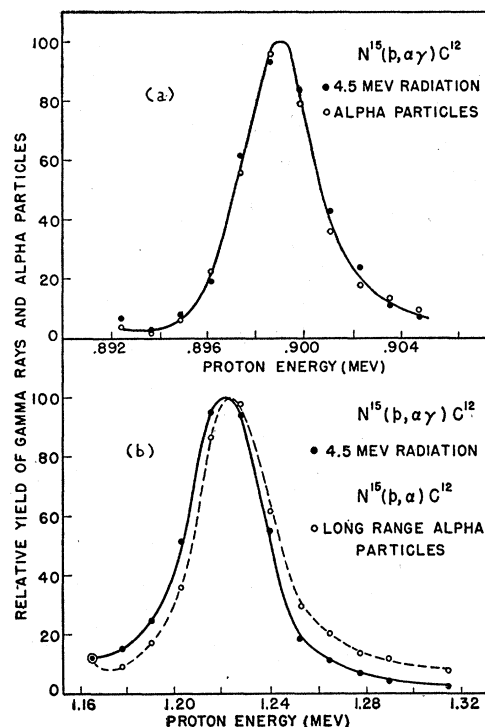


FIG. 4. (a) Excitation curve of alpha-particles and gamma-rays of $N^{15}(p, \alpha \gamma)C^{12}$ at the 0.898-Mev resonance. (b) Displacement of the excitation of gamma-radiation and long-range alpha-particles at the 1.210-Mev resonance. A 30 kev (at 0.90 Mev) target was used.

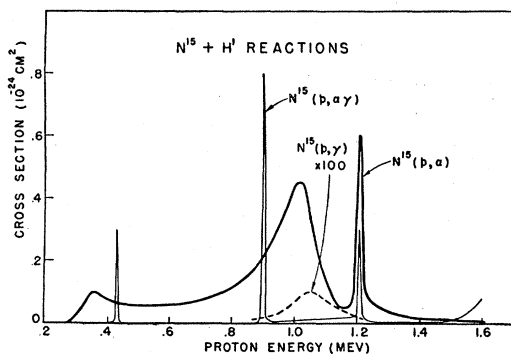


FIG. 5. Schematic excitation curves for the $N^{15}+H^1$ reactions. (The width of the narrow resonances are not shown to scale.)

Figure 6 shows the excitation curve for long-range alpha-particles. The measurements with the spectrograph showed that their energy agrees within 0.1 Mev with the energy to be expected for reaction (1) using masses given by Li *et al.*²⁰ The alpha-particles observed with the proportional counter had an energy greater than 3 Mev. No increase in counts was observed if all alpha-particles with energy greater than 2.2 Mev were counted. The yield was also linear in the N^{15} content of the target.

Figure 7 was prepared from gamma-ray measurements. In addition, thick and thin target curves were taken at the various resonances. Coincidence absorption measurements at the resonances show primarily 4.5-Mev radiation. At the 1.210-Mev resonance Thomas and Lauritsen²¹ measured the quantum energy with a β -ray spectrometer and obtained 4.465 ± 0.020 Mev, but a Doppler correction may reduce this value by as much as 0.020 Mev to 4.445 Mev (private communication). Strait, *et al.*²² measured 4.960 ± 0.007 Mev for the Q -value of $N^{14}(p, \alpha)C^{12}$, while Li *et al.*²⁰ give 4.961 ± 0.006 Mev. The excitation of the lowest excited state of C^{12} is thus $4.961 - 0.529 = 4.432 \pm 0.010$ Mev.

Around 1.05 Mev, coincidence absorption measurements show the presence of some 13-Mev radiation. Capture radiation to the ground state in O^{16} is the only process which is sufficiently energetic. The other part of the radiation is probably mostly 4.5 Mev. Unfortunately the measurements are not very energy sensitive, and a large fraction of 6- or 7-Mev quanta cannot be ruled out. One would expect radiation in this energy range if cascading occurs in some of the capture radiation. Thus the 4.5-Mev component may be smaller in the 0.95- to 1.2-Mev region than has been shown on the graph.

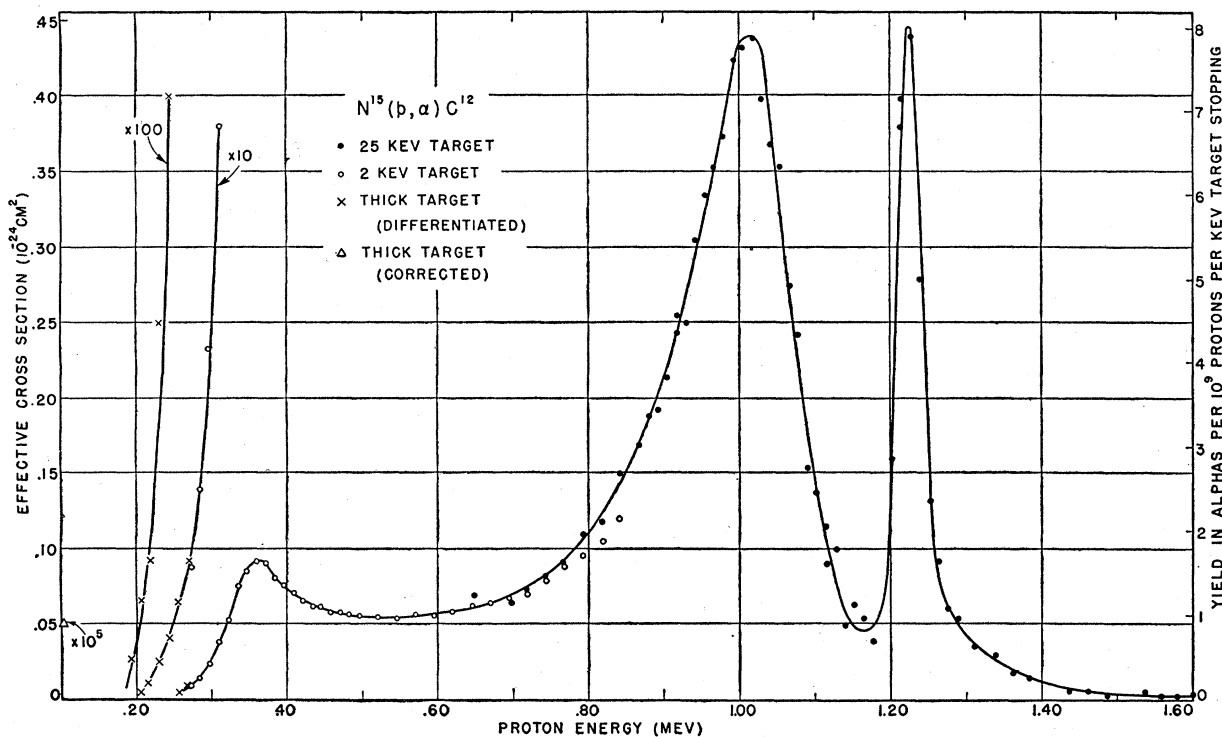


FIG. 6. Excitation curve of long range alpha-particles. The angle of observation is 90° for points designated by open circles and crosses, 137.8° for points designated by solid circles. The yield is given for a KNO_3 target enriched to 61 percent with N^{15} . Target thickness distorts the curve only at the 1.21-Mev resonance.

²⁰ Li, Whaling, Fowler, and Lauritsen, Phys. Rev. **83**, 512 (1951).

²¹ R. G. Thomas and T. Lauritsen (to be published).

²² Strait, Van Patter, Buechner, and Sparduto, Phys. Rev. **81**, 747 (1951).

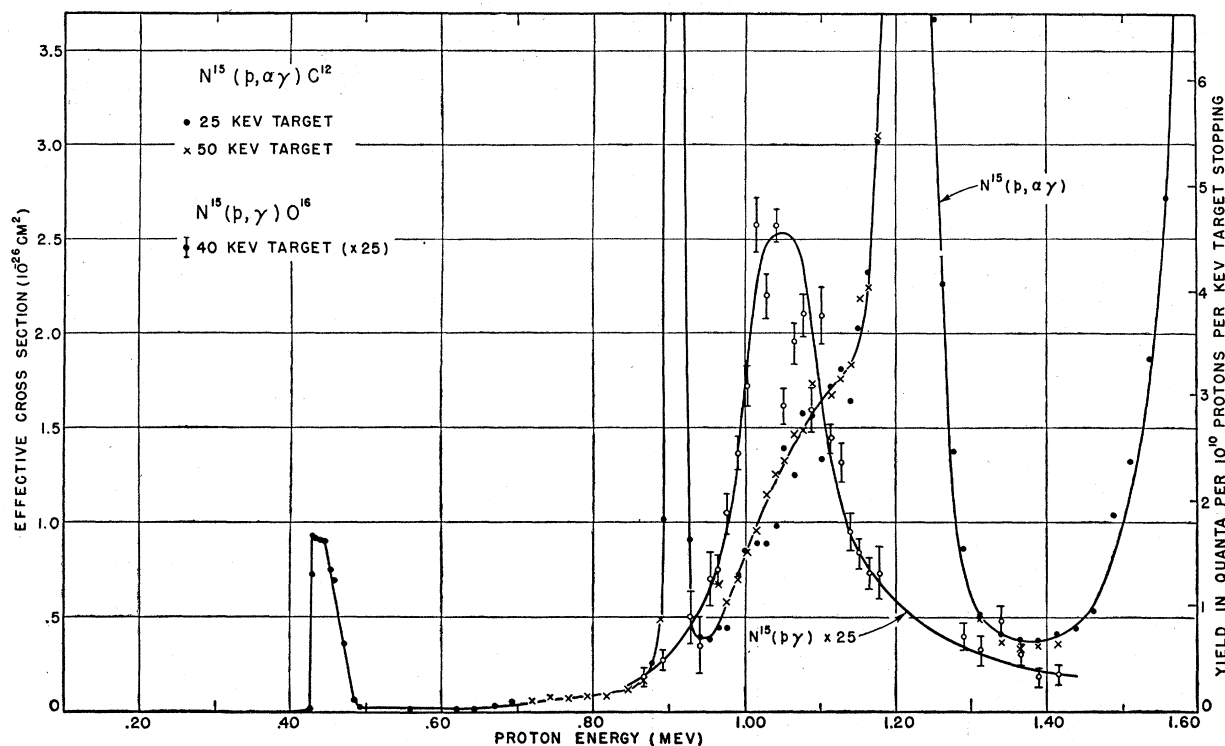


FIG. 7. Excitation curve of gamma-radiation. All measurements were made at 90° . The yield is given for a KNO_3 target enriched to 61 percent with N^{15} .

Since the target contained other nuclei besides N^{15} , one has to check whether any of them influence the measurements. Both KNO_3 and TiN targets were used above 0.4 Mev. The results agree if the variation of nitrogen concentration with depth in the TiN target is taken into account. At the bombarding energies used, the Coulomb barrier of both titanium and potassium is large; therefore, their transmutation cross sections are small. The $N^{14}+H^1$ cross sections have been investigated by Duncan and Perry²³ and were found to be much smaller than the N^{15} cross sections. For $N^{14}(p, \gamma)O^{15}$ the largest resonance is at 1.065 Mev, with a cross section of $3.5 \times 10^{-28} \text{ cm}^2$ and $\Gamma = 5 \text{ kev}$. Thus, it is about $\frac{1}{3}$ of the $N^{15}(p, \gamma)O^{16}$ cross section, but because of its small width the yield was negligible compared to the N^{15} reaction. Blank runs with normal KNO_3 showed no detectable gamma-radiation. For the measurements below 0.4 Mev, special care was taken to eliminate B^{11} contaminations. All measurements were reproducible in both yield and position of resonances.

As can be seen from Fig. 5 most of the resonances of the short- and long-range alpha-particles are not common. The 1.210-Mev resonance, however, is common to both reactions. Figure 4(b) shows the yields of the two reactions plotted on a relative scale. Since both yields were measured together, the displacement of a few kev is real and will be discussed below. The cross section curve (Fig. 7) for the short-range alpha-particles

indicates a small resonance between 1.0 and 1.1 Mev which is masked by the tail of the 1.210-Mev resonance.

To interpret these excitation curves in terms of energy levels it is necessary to use a Breit-Wigner multi-level dispersion formula. Unfortunately a knowledge of the angular distribution of the cross sections is necessary. With the results obtained until now, one is limited to the single level formula applied at each resonance plus the possibility of interference terms.

The single level formula is

$$\sigma = \pi \lambda^2 \frac{\omega \Gamma_p \Gamma_x}{(E - E_R)^2 + \Gamma^2/4}, \quad (5)$$

where λ is the wavelength of the incident proton in the c.m. system, Γ_p the proton width, Γ_x the width of emitted radiation, Γ the full width at half maximum of the resonance, E and E_R are the proton energy and resonance energy, respectively, ω is a statistical factor given by $\omega = (2J+1)/(2s+1)(2i+1)$, J is the total angular momentum of the compound nucleus, s and i are the spins of the incident and target nucleus, respectively. Γ_p and Γ_x are not constant due to the barrier penetration factors. In the notation of Christy and Latter²⁴ $\Gamma = (E/E_1)^{1/2} PG$. Here P is the Gamow penetration factor. $(E/E_1)^{1/2}$ gives the velocity normalization. G is the width without barrier at a velocity of 1.4×10^9

²³ D. B. Duncan and J. E. Perry, Phys. Rev. 80, 136 (1950).

²⁴ R. F. Christy and R. Latter, Revs. Modern Phys. 20, 185 (1948).

cm-sec, provided $E_1=1$ Mev for protons and 4 Mev for alpha-particles.

The dispersion formula is most easily applied to the narrow resonances of the $N^{15}(p,\alpha\gamma)C^{12}$ reaction. Here the variation of penetration factors over the resonance width is negligible. The nonresonant radiation is small, thus interference terms are not important; the wide resonances of $N^{15}(p,\alpha)C^{12}$ are not as readily interpreted. The proton penetration factor changes greatly over the resonance width and interference effects between resonances become noticeable. As a first step, the cross section (Fig. 6) was divided by the proton Gamow factor and $4\pi\lambda^2$. Then Eq. (5) takes the following form:

$$\frac{\sigma}{4\pi\lambda^2(E/E_1)^{1/2}P} = \frac{\frac{1}{4}\omega G_p \Gamma_\alpha}{(E-E_R)^2 + \frac{1}{4}\Gamma^2} \quad (6)$$

Since the alpha-particle energy is larger than the

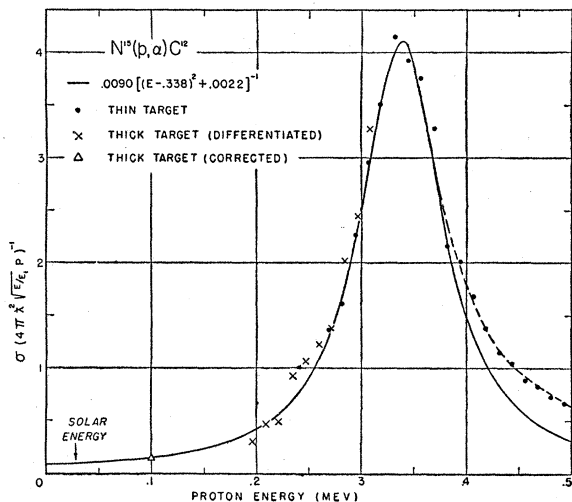


FIG. 8. Excitation curve of long-range alpha-particles after barrier factors have been divided out (s-wave protons were assumed).

potential barrier, Γ_α may be considered constant. In Fig. 8 we plot experimental points representing the quantity given on the left-hand side of Eq. (6). The values for P were taken from the curves of Christy and Latter for s-wave protons incident on nitrogen.²⁵ As shown in the figure the experimental points below 0.4 Mev can be fitted by a resonance curve (right-hand side of Eq. (6) with the maximum at 0.338 Mev and a width of 94 kev. The agreement is rather remarkable considering the change in cross section from 0.09 barn at 0.360 Mev to 5×10^{-7} barn at 0.100 Mev.

Above 0.4 Mev, however, the experimental points start to deviate markedly from the resonance curve. The asymmetry of the next resonance, at about 1 Mev, is even more marked after a penetration factor is taken out. This behavior can be explained by interference

between the three long-range alpha-particle resonances. Constructive interference between the low and 1-Mev resonances is indicated in the region from 0.4 to 1 Mev (Figs. 6 and 8). Since there is a phase shift of 180° in going through a resonance, the interference is destructive below 0.3 and above 1 Mev. Interference between the 1.0 and 1.2 Mev resonances may explain the slight displacement between the maxima of the long-range alpha-particle and gamma-ray yield at the 1.210-Mev resonance [Fig. 4(b)], and may also explain the surprisingly low value of the cross section at 1.6 Mev. Single level dispersion formulas were approximately fitted at the three resonances. The effect of interference terms can be estimated by taking differences of the amplitudes. The analysis showed that interference effects can be quite large. The true resonance position of the 1-Mev resonance in the long-range alpha-particles could be shifted to a considerably higher or lower energy. Until phase factors are accurately taken into account no quantitative calculation is possible.

Between 1.0 and 1.1 Mev all three reactions show resonance phenomena (Figs. 6 and 7). The widths are about 150 kev, although none of them can be measured very accurately. The present data are consistent with the assumption that all three correspond to only one state in O^{16} . We assume that the capture radiation gives the true position of the resonance, 1.05 Mev, and we quote this value for all three reactions. The maximum of the long-range alpha-yield is displaced toward lower energies by the interference with the 1.210-Mev resonance. The maximum of the short-range alpha-particles is displaced toward higher energies by the penetration factor of the alphas. The exact position and width of this resonance is masked by the tail of the 1.210-Mev resonances.

The pertinent experimental information about the resonances has been summarized in Table I. The thick target yield is given only for the narrow resonances. The $N^{15}(p,\alpha\gamma)$ resonance above 1.6 Mev has not been included. The gamma-ray yield was rising rapidly at the highest energy available. The long-range alpha-particles do not participate in this rise.

The data from Table I can be used to calculate the nuclear width without barrier, Γ , provided the statistical weight of the levels involved is known. Then by the usual intensity arguments, it is possible to limit the angular momentum and parity assignments of the states involved. This was done by one of the authors.²⁶ It was possible to find selection rules which determined whether the resonances were common between reactions (1), (2), and (3) or not.²⁷

The Γ_γ involved for the capture radiation at the 1.05-Mev resonance indicates that it is an electric

²⁶ A. W. Schardt, Ph.D. thesis, California Institute of Technology (1951).

²⁷ Note added in proof:—For example, states in O^{16} with angular momentum and parity given by $0^-, 1^+, 2^- \dots$ cannot decay by long-range alpha-particle emission.

²⁵ In the low energy region it makes very little difference which partial wave is used.

dipole transition. In that case one would expect very little cascading through the 6.13-Mev levels in O¹⁶, but about 10 percent cascading through the pair state at 6.05 Mev. On the other hand, if the 13-Mev radiation is electric quadrupole, then considerable cascading through the 6.13-, 6.9-, and 7.1-Mev level is to be expected. Unfortunately the pairs could not be detected since a thick Al converter was used and the experimental results are not sufficiently accurate to determine the amount of cascading.

VIII. EXTRAPOLATION TO STELLAR ENERGIES

For stellar energy production only the value of the cross sections around 30 kev is important. This can be estimated by extrapolating as shown in Fig. 8. At low energies the tail of the cross section curve is given approximately by

$$\sigma_{\alpha}(E) = (110/E) \exp(-6.95E^{-1/2}), \quad (7)$$

where σ_{α} is in barns provided E is in Mev. This yields $\sigma_{\alpha} = 1.5 \times 10^{-14}$ barns at 30 kev.

The above expression would be quite accurate except for two facts. The amplitudes at 30 kev contributed by the 1.05-Mev resonance and the 0.338-Mev resonance are comparable. The interference of the two amplitudes is probably destructive and the value given in Eq. (7) may be high by a factor of 2. Furthermore, from the present experiments no information can be gained regarding resonances below 0.1 Mev and Eq. (7) assumes that none exist. Thus $\sigma_{\alpha} = 1.5 \times 10^{-14}$ barns at 30 kev is consistent with the present observations but may be considerably in error if a low-lying resonance exists.

Compared to N¹⁵(p, α)C¹², the N¹⁵($p, \alpha\gamma$)C¹² reaction gives no appreciable contribution to stellar energy production. Its main resonances are very narrow (Table I) and no nonresonant radiation was found. An extrapolation of the N¹⁵(p, γ)O¹⁶ cross section to stellar energies is of interest, because this process removes

nitrogen permanently from the carbon cycle. The reaction could be observed only at the 1.05-Mev resonance, because its yield is small. There is no reason to suppose, however, that it does not have other resonances. For instance, it may compete with the long-range alpha-particles at the 0.338-Mev resonance. This could not have been detected in laboratory measurements, but might make a significant contribution at 30 kev in stars.

In extrapolating from 1.05 Mev to 0.03 Mev it is important to use the correct incident proton wave. This resonance is probably also due to s -wave protons.²⁶ Equation (5) was used in the extrapolation. In order to obtain a minimum estimate $\Gamma = 135$ kev was used. This together with values given in Table I gives

$$\sigma_{\gamma}(E) = (0.009/E) \exp(-6.95E^{-1/2}). \quad (8)$$

This is only the contribution of one resonance, and the

TABLE I. Resonance data.

Resonance energy (Mev)	Γ kev	$\sigma(p, \alpha)$ barns	$\sigma(p, \alpha\gamma)$ barns	$Y(p, \alpha\gamma)$ quanta/proton ^a	$\sigma(p, \gamma)$ barns
0.338 ^b	94	0.075
0.429 \pm 0.001	0.9	...	0.3	4 \times 10 ⁻⁹	...
0.898 \pm 0.001	2.2	...	0.8	5 \times 10 ⁻⁸	...
1.05 ^c	\sim 150	0.5	0.015	...	0.001
1.210 \pm 0.003 ^d	22.5 ^d	0.6	0.3	1.8 \times 10 ⁻⁷	...

^a Yield is for thick KNO₃ target containing 61 atom percent of N¹⁵.

^b Experimental data has been corrected for s -wave penetration factor.

$E_{\max} = 0.36$ Mev, $\sigma_{\max} = 0.09$ barn.

^c This value taken from the N¹⁵(p, γ) resonance.

^d These values were measured from the $\sigma(p, \alpha\gamma)$ curve and may be different for $\sigma(p, \alpha)$.

actual value of σ_{γ} is probably larger. Combining Eqs. (7) and (8), one gets $\sigma_{\gamma}/\sigma_{\alpha} \geq 0.8 \times 10^{-4}$. This value is larger than assumed by Bethe⁶ but is still small enough not to interfere with the carbon cycle during the age of the sun.

The authors want to express their gratitude to Professors R. F. Christy and T. Lauritsen for many discussions during the course of this research.